Di-trinucleon resonance states of $A = 6$ systems in a microscopic cluster model

K. Arai,[1,*] K. Katō,[2] and S. Aoyama[3]

[1]*Division of General Education, Nagaoka National College of Technology, 888 Nishikatakai, Nagaoka, Niigata, 940-8532, Japan*

[2]*Division of Physics, Graduate School of Science, Hokkaido University, Sapporo 060-0810, Japan*

[3]*Integrated Information Processing Center, Niigata University, Niigata 950-2181, Japan*

(Received 24 May 2006; published 6 September 2006)

Highly excited resonance states lying above the $t+t$ threshold in ^{6}He are theoretically studied by the $t+t$ microscopic two-cluster model. The $t+t$ two-body scattering problem is solved by the microscopic R-matrix method in order to localize resonance states. Excited states of ^{6}Be and ^{6}Li (both $T = 1$ and 0) are as well studied within the consistent two-cluster models. We have employed four different effective nucleon-nucleon interactions in order to check the sensitivity to our results and we have obtained fairly consistent results in every interaction. In positive parity states, our model gives deeply bound states which are well-known low-lying $\alpha+n+n$ three-body states and these states are obtained through the overlap between the $t+t$ and $\alpha+n+n$ configurations at smaller cluster relative distance. Similar bound states are found in the $T = 0$ state in ^{6}Li. In negative parity states, our calculation shows broad 0^- and 2^- P-wave resonances just above the $t+t$ threshold and in addition three F-wave resonances of 2^-, 3^-, and 4^- at higher energies with broader widths. Our calculations show that the noncentral term of the effective nucleon-nucleon interaction plays an important role for these broad resonance states. $T = 0$ states of ^{6}Li show single broad resonances in P- and F-waves, respectively, and their positions are very close to those of $T = 1$ resonances.

DOI: 10.1103/PhysRevC.74.034305 PACS number(s): 21.45.+v, 21.60.Gx, 25.70.Ef, 27.20.+n

I. INTRODUCTION

The neutron rich nucleus ^{6}He has drawn strong attractions due to its exotic structure such as the neutron halo in the ground and excited states [1]. Various theoretical and experimental studies prove that the ground and low-lying excited states have a good $\alpha+n+n$ three-body structure. On the other hand, the highly excited states more than 12 MeV could have another exotic aspect in the ^{6}He structure because the $t+t$ channel comes to be another opened channel together with the $\alpha+n+n$ at $E_x = 12.3$ MeV [2].

Experimentally, Akimune and co-workers [3] studied recently highly excited states of ^{6}He and found a di-triton resonance at $E_x = 18.0\pm1.0$ MeV with $\Gamma_R = 9.5 \pm 1.0$ MeV as a P-wave resonance. As for resonance states in ^{6}Li and ^{6}Be, a number of experimental efforts were so far performed in order to determine P- and F-wave resonances above two-body threshold but some disagreements in the resonance parameters were found among their measurements [4–6]. Most recent experiments in Ref. [3] reported a $T = 1$ P-wave resonance at $E_x = 18.0\pm1.2$ MeV with $\Gamma_R = 9.2\pm1.3$ MeV in ^{6}Be and at $E_x = 22.0 \pm 1.0$ MeV with $\Gamma_R = 8\pm1$ MeV in ^{6}Li. And they reported at $E_x = 18.0 \pm 0.5$ MeV with $\Gamma_R = 5.0 \pm 0.5$ MeV as a $T = 0$ P-wave resonance in ^{6}Li.

Theoretically, in a few decades ago, Thompson and Tang [7] studied the di-trinucleon resonances in $A = 6$ nuclei with the resonating group method (RGM) [8,9] and showed P- and F-wave resonances. More recently, Ohkura *et al.* [10] employed the complex scaling method (CSM) [11,12] in the RGM calculation in order to localize these broad P- and F-wave resonance states in ^{6}Li. It is to be noted that their calculations neglected the spin-orbit and tensor terms of the interaction whereas these are essential to know the spin-parity and width of the P- and F-wave resonances. Since the triton has a spin and parity of $1/2^+$, the spin-orbit and tensor forces split the P- and F-waves to three states, respectively. In the present paper, therefore, we have added the spin-orbit and tensor terms to the effective nucleon-nucleon interaction with the aim of discussing the spin-parity of the $t+t$ clustering resonance.

In ^{6}He, the soft dipole resonance (SDR) [13,14], which is a dipole oscillation of an α-cluster core against valence neutrons, has been hotly discussed experimentally [15] and theoretically [16–18] as one of most intriguing topics. Theoretically, a very recent calculation in the $\alpha+n+n$ three-body model by Aoyama [19] showed that this SDR with a spin-parity of 1^- could have an excessively large decay width ($\Gamma_R = 31.2$ MeV) than expected. In connection with this SDR, it might have a certain importance to know the spin-parity of the $t + t$ P-wave resonance since both resonances might affect, if it is 1^-, their resonance positions each other through some coupling effect. And it could put a necessity on the theoretical study to perform a coupled channel calculation of the $\alpha+n+n$ and the $t+t$ systems in order to confirm theoretically the SDR in ^{6}He. Note that, in the ground 0^+ state, an additional $t+t$ channel on the three-body calculation is known to be non-negligible in order to reproduce its binding energy [20,21]. However, we concentrate our discussion on only the $t+t$ clustering resonance in the present paper because an explicit treatment of a three-body resonance including the two-body channel is much difficult in our model and the SDR itself is out of the scope in present theoretical study.

*Electronic address: arai@nagaoka-ct.ac.jp

In the present theoretical study, we have employed the t+t microscopic cluster model of the type of the RGM as was used in the preceding theoretical studies. The two-body scattering problem is solved by the means of the microscopic R-matrix method [22,23] and parameters of the di-triton resonances are directly derived from the position of the S-matrix pole at the complex energy (momentum) plane. As for the effective nucleon-nucleon interaction to be used in the present RGM calculation, we have tried four different interactions, all of which include the spin-orbit and tensor terms, in order to know the sensitivity of the resonance parameters to the choice of the interaction. Other members of the isobaric analog states of $T = 1$ resonances in ^{6}Li and ^{6}Be have been studied as well and in addition the $T = 0$ resonance in ^{6}Li has been searched with the consistent t+h model.

II. MODEL

In the present study of $A = 6$ nuclei, we employed a $(3N)$+$(3N)$ two-body microscopic cluster model according to the RGM. In this method, the nucleons are assumed to be arranged in $0s$ clusters and all nucleons are treated explicitly. The wave function is constructed to satisfy the Pauli principle for all nucleons exactly and is free from spurious center-of-mass motion while also having good total angular momentum and parity. The intrinsic wave functions of the t and h are taken to be simple shell-model wave functions built up from a single $0s$ harmonic-oscillator state.

The wave function can be obtained approximately by solving the six-nucleon Schrödinger equation in which the six-nucleon Hamiltonian has an effective nucleon-nucleon interaction. In this study, we have tried four different effective N-N interactions so as to check the sensitivity of our results to the choice of the effective interactions. The first interaction is the Minnesota potential ($u = 0.98$) [24] with the spin-orbit term of Reichstein and Tang (set number IV) [25] and the tensor term of Heiss and Hackenbroich [26]. This Minnesota potential with the tensor term was employed by Csótó for the studies of the light nuclei [27]. The second interaction is by Csótó and Lovas [28], which was used to calculate the ground state of ^{6}Li. The third is by Furutani *et al.* [29] and the fourth is by Mertelmeier and Hofmann [30]. These are hereafter denoted by MN, CL, FU, and MH, respectively.

The total wave function with total angular momentum J and parity π is given in the RGM as

$$\Psi^{JM\pi} = \mathcal{A}\{[[\Phi^i \Phi^j]_{ST}\ \chi_\ell(\boldsymbol{\rho})]_{JM}\}, \tag{1}$$

where Φ^i is an intrinsic wave function of ^{3}H(t) or ^{3}He(h) clusters and the superscript (i, j) means (t, t) for ^{6}He, (h, h) for ^{6}Be, and (t, h) for ^{6}Li. $\chi_\ell(\boldsymbol{\rho})$ is the cluster relative wave function with the partial wave ℓ and $\boldsymbol{\rho}$ denotes the cluster relative coordinate. The symbol $\mathcal{A}$ is the intercluster antisymmetrizer. S and T are the total spin and isospin, respectively. In $T = 1$ states, the Pauli principle allows only $S = 0$ for the positive parity state and only $S = 1$ for the negative parity state, while $T = 0$ states allow only $S = 1$ for the positive parity state and $S = 0$ for the negative parity state. The size parameter of the triton cluster is set to minimize the triton binding energy with a single $(0s)^3$ function and the same parameter is used for the ^{3}He cluster. The size parameters used for MN, CL, FU, and MH potentials are $\nu =$ 0.2255 fm^{-2}, 0.185 fm^{-2},0.23 fm^{-2}, and 0.255 fm^{-2}, respectively. These parameters give the energy (rms radius) of the triton as -4.56 MeV (1.49 fm), -7.46 MeV (1.64 fm), -6.71 MeV (1.47 fm), and -6.40 MeV (1.40 fm), respectively, while the experimental energy is -8.48 MeV [31]. And the energy of ^{3}He is given as -3.79 MeV, -6.77 MeV, -5.93 MeV, and -5.58 MeV, respectively, while the experimental energy is -7.72 MeV [31]. We should note that the present model does not take into account the cluster distortion effect [28] which could be given by the the superposition of the $(0s)^3$ function with various size parameters. Although such an effect could affect the resonance parameters of the t+t resonance to a certain extent, we have compromised to employ the single $(0s)^3$ function because such a superposition makes difficult to remove the center-of-mass motion from the present wave function. But this uncertainty by the neglecting the distortion effect is unlikely to be much larger than that by the choice of the effective interaction.

The cluster relative motion is solved by the microscopic R-matrix method where the wave function inside the channel radius is approximated by the superposition of the various range of the Gaussian basis function as given in Eqs. (4) and (5) in Ref. [32] and is connected with the Coulomb function at the channel radius [22,23]. Since the resonance states to be calculated are possibly broad resonances according to the preceding experimental and theoretical studies, in order to obtain the resonance parameters accurately, we have employed an analytic continuation of the S-matrix to the complex energies (ACS) [27] in which the S-matrix is calculated at a complex energy(momentum) using the Coulomb functions at complex momenta as described in Ref. [33] and the resonance parameters are directly given by the position of the S-matrix pole as $E = E_R - i\Gamma_R/2$.

Above $E_x = 12.3$ MeV in ^{6}He, not only the t+t channel but also the α+n+n channel come to be opened channels, therefore a rigorous argument for continuum states above the t+t threshold requires to include both channels simultaneously while such a complicated calculation for continuum states is not feasible in our model at the present moment. We take into account only the t+t channel in the present study since our aim of the present calculation is to discuss the resonance states with the t+t clustering rather than to discuss generally continuum states and the t+t model without the α+n+n channel could have enough reliability if we discuss only the t+t clustering resonance in ^{6}He.

III. RESULTS AND DISCUSSIONS

Phase shifts of the t+t elastic scattering for positive parity states with the MN potential are shown in Fig. 1 wherein the solid line exhibits the 0^+ ($^1S_0$) phase shift and the dashed line 2^+ ($^1D_2$). As seen from this figure, the positive parity states (0^+ and 2^+) do not give any sign of resonance in calculated elastic phase shifts at the low energy region and this result is consistent with those in Ref. [7]. It is noted that the phase

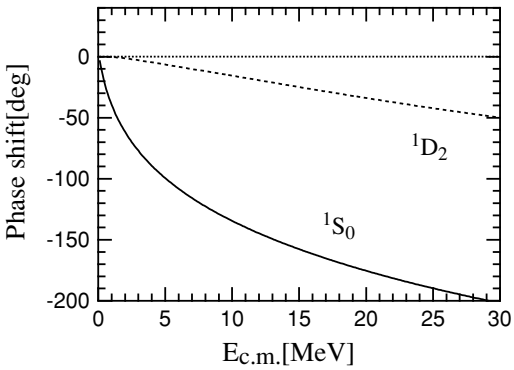

FIG. 1. t+t elastic phase shifts for the positive parity states in ^{6}He. The MN potential is used for effective N-N potential. These are given as a function of the c.m. energy with respect to the t+t threshold. The phase shifts of $^1S_0$ and $^1D_2$ are given by the solid and dotted lines, respectively.

shifts with the CL, FU, and MH potentials do not give any significant difference from those with the MN potential.

In Fig. 2, the phase shifts for negative parity states are shown. In the negative parity states, we can consider six states for the $T = 1$ channel: $[L = 1 \otimes S = 1]_{J^\pi=0^-,1^-,2^-}$ and $[L = 3 \otimes S = 1]_{J^\pi=2^-,3^-,4^-}$. These six phase shifts of $^3P_0, ^3P_1, ^3P_2, ^3F_2, ^3F_3$, and $^3F_4$ are given in Fig. 2 by solid, dotted, dashed, dash-dotted, dash-double-dotted, and long-dashed lines, respectively. As shown in Fig. 2, the low energy peaks of the P-wave (solid and dashed lines) and F-wave phase shifts suggest an existence of several broad resonances. The order of the phase shifts in both waves is not sensitive at all to the choice of the effective N-N interaction. In P-wave states, every interaction indicates very broad resonances just above the threshold. The 0^- state shows the most prominent peak among the P-wave phase shifts and the 2^- resonance could lie close to the 0^- resonance but with a much broader width. The position of these resonances are not much sensitive to the choice of the interaction but their widths are more sensitive to. As for the 1^- states, the t+t relative interaction is much less attractive than in other two states. Because a peak of the calculated phase shifts for 1^- does not reach more than 5° for all the interactions, it could not be observed experimentally as a resonance. Therefore, 0^- or 2^- or a mixture of them is a candidate for the recently observed P-wave resonance above the t+t threshold [3]. Note that this order (0^-, 2^-, and 1^-) of the P-wave splitting is decisively attributed to the tensor force between the two clusters. Similar trend is seen in the P-wave low energy phase shifts of p+p [20,27]. Without the tensor force, the order of the P-wave splitting is naturally 2^-, 1^-, and 0^- due to the spin-orbit force but the tensor force gives a more attractive effect in the 0^- state and a more repulsive effect in the 1^- state.

In F-wave states of 2^-, 3^-, and 4^-, each phase shift explicitly shows the broad resonance behavior at energies higher than those of the P-wave resonances. And their resonance parameters are not strongly sensitive to the choice of the interaction except the CL potential as shown later

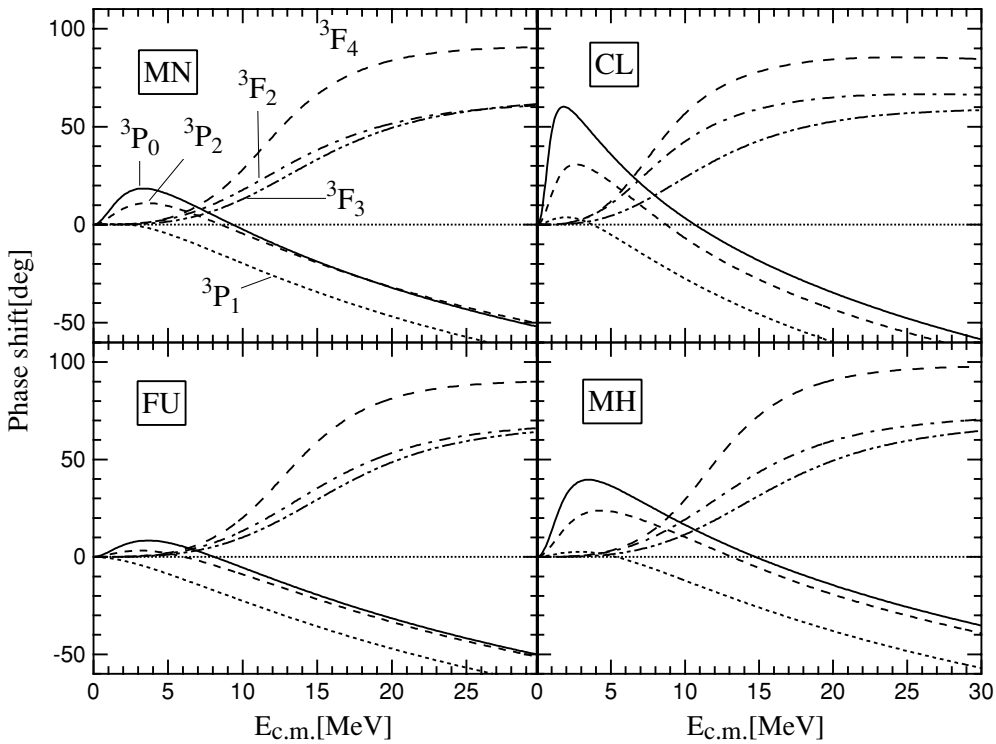

FIG. 2. t+t elastic phase shifts for the negative parity states in ^{6}He. The phase shifts of $^3P_0, ^3P_1, ^3P_2, ^3F_2, ^3F_3$, and $^3F_4$ are given by the solid, dotted, dashed, dash-dotted, dash-double-dotted, and long-dashed lines, respectively. MN, CL, FU, and MH distinguish the employed effective N-N interaction as is given in the text.

TABLE I. Resonance parameters of ^{6}He, ^{6}Li ($T = 1, 0$), and ^{6}Be. MN potential [24–26] is employed as the N-N interaction. E_R and Γ_R are the resonance energy relative to respective two-body threshold and resonance width, respectively. Unit is given in MeV. Value in the parenthesis at Γ_R presents rms radius (fm) in bound state.

$T = 1$	^{6}He		^{6}Li		^{6}Be	
J^π	E_R	Γ_R	E_R	Γ_R	E_R	Γ_R
0^+	−6.09	(2.10)	−5.72	(2.10)	−4.75	(2.12)
2^+	−4.67	(2.01)	−4.29	(2.01)	−3.38	(2.02)
0^-	0.6	4.2	0.9	4.6	1.5	5.4
$2^-(\ell = 1)$	0.3	5.8	0.6	6.3	1.3	7.2
$2^-(\ell = 3)$	11	18	11	19	12	20
3^-	12	19	13	19	14	20
4^-	11	11	12	12	13	12
$T = 0$						
1^+			−11.81	(1.96)		
			−0.02	(2.42)		
2^+			−6.83	(1.99)		
3^+			−11.03	(1.90)		
1^-			0.3	6.7		
3^-			12	16		

TABLE III. Resonance parameters of ^{6}He, ^{6}Li ($T = 1, 0$), and ^{6}Be. FU potential [29] is employed as the N-N interaction. For notation, see Table I.

$T = 1$	^{6}He		^{6}Li		^{6}Be	
J^π	E_R	Γ_R	E_R	Γ_R	E_R	Γ_R
0^+	−8.07	(2.02)	−7.69	(2.02)	−6.68	(2.03)
2^+	−6.17	(1.96)	−5.79	(1.96)	−4.85	(1.96)
0^-	0.1	6.6	0.5	7.1	1.3	8.1
$2^-(\ell = 1)$	−0.6	8.2	−0.3	9	0.6	10
$2^-(\ell = 3)$	13	18	13	18	14	19
3^-	14	19	15	19	16	20
4^-	13	11	13	12	14	12
$T = 0$						
1^+			−12.06	(1.94)		
			−2.16	(2.08)		
2^+			−8.15	(1.95)		
3^+			−11.75	(1.88)		
1^-						
3^-			17	22		

(Tables I–IV). These three F-wave resonances concentrate within 1–2 MeV, and the 4^- state (long-dashed line) is a slightly narrower one whereas the other two states have similar widths each other.

It might be interesting to note that the order of P-wave states (0^-, 2^-, and 1^-) is different from that (2^-, 1^-, and 0^-) of the shell model in Ref. [34] wherein the 0^- state has much higher energy than the other two states. And, in F-waves, the 3^- state has much higher energy than the second 2^- and 4^- states in Ref. [34] whereas our model gives a small difference in their positions as written above. And note that these odd states must be, in the shell model configuration, given by the $1\hbar\omega$ excitation, where one nucleon in the p-shell excites into the sd-shell or one in the s-shell excites into the p-shell. Although the odd-wave t+t clustering state implies the s-hole dominance in the shell model configuration [10], it is known that the shell model requires much higher excitation in order to reproduce accurately a cluster model wave function for a developed clustering state [36].

The resonance parameters of $T = 1$ states obtained by the ACS for the different N-N interactions are given in an upper part of Tables I–IV. The left, middle and right columns in the tables are the calculated resonance energies and the decay widths for ^{6}He, ^{6}Li, and ^{6}Be, respectively. For bound states,

TABLE II. Resonance parameters of ^{6}He, ^{6}Li ($T = 1, 0$), and ^{6}Be. CL [27]is employed as the N-N interaction. For notation, see Table I.

$T = 1$	^{6}He		^{6}Li		^{6}Be	
J^π	E_R	Γ_R	E_R	Γ_R	E_R	Γ_R
0^+	−8.92	(2.25)	−8.58	(2.25)	−7.67	(2.26)
2^+	−6.58	(2.20)	−6.24	(2.20)	−5.40	(2.21)
0^-	0.6	1.1	0.9	1.4	1.4	1.9
$2^-(\ell = 1)$	0.7	2.6	0.9	2.9	1.5	3.5
$2^-(\ell = 3)$	6	12	6	12	7	12
3^-	8	16	9	17	9	18
4^-	7	9	7–8	9–10	8	10
$T = 0$						
1^+			−8.32	(2.27)		
			−0.47	(2.41)		
2^+			−6.99	(2.22)		
3^+			−7.79	(2.16)		
1^-			0.8	3.5		
3^-			8	13		

TABLE IV. Resonance parameters of ^{6}He, ^{6}Li ($T = 1, 0$), and ^{6}Be. MH potential [30] is employed as the N-N interaction. For notation, see Table I.

$T = 1$	^{6}He		^{6}Li		^{6}Be	
J^π	E_R	Γ_R	E_R	Γ_R	E_R	Γ_R
0^+	−9.29	(1.92)	−8.90	(1.92)	−7.84	(1.93)
2^+	−6.93	(1.87)	−6.52	(1.87)	−5.54	(1.87)
0^-	0.9	3.0	1.3	3.3	1.9	4.1
$2^-(\ell = 1)$	0.9	4.9	1.2	5.3	1.9	6.2
$2^-(\ell = 3)$	11	17	11	17	12	18
3^-	13	19	14	19	15	20
4^-	11	10	12	10	13	11
$T = 0$						
1^+			−14.32	(1.85)		
			−2.22	(1.99)		
2^+			−10.23	(1.86)		
3^+			−14.58	(1.79)		
1^-			0.9	6.1		
3^-			13	15		

we give the rms radii in the parenthesis instead of the decay widths. For positive parity states, our two-cluster model gives two deeply bound states of $J^\pi = 0^+$ and 2^+ as shown in Tables I–IV, while no bound state is found in negative parity state. Both in experimentally and theoretically, ^{6}He is well known to have the 0^+ and 2^+ states as the ground and the first excited ($E_x = 1.8$ MeV [2]) states, respectively, where both states are understood to have a good $\alpha+n+n$ three-body structure. Note that the $t+t$ threshold lies experimentally at $E_x = 12.3$ MeV [2]. When the cluster relative distance is smaller, two different configurations, $\alpha+n+n$ and $t+t$, can have larger overlap each other, therefore these two bound states can be regarded as well-known low-lying three-body states rather than the $t+t$ bound states. Regarding this overlap, Csótó already discussed the large overlap between $\alpha+n+n$ and $t+t$ in the ground state [20]. In order to confirm this idea, we calculate the $t+t$ reduced width amplitude in these two states and our results give one node for the S-wave state (0^+) and zero node for the D-wave state (2^+) meaning that these two states are dominated by $0\hbar\omega$ excitation in the shell model configuration. In addition, the shape of the amplitude in this 0^+ state is quite similar with that obtained by the three-cluster model [21]. Therefore these results confirm the above conclusion concerning these bound states. It should be stressed that the wave functions obtained by the $t+t$ model can produce a mere certain part of these states since these bound states are obtained simply through the overlap between two different configurations and therefore these wave functions are insufficient to replace the $\alpha+n+n$ wave functions.

As far as the negative parity states in Tables I–IV are concerned, the 0^- and 2^- states are obtained as the P-wave resonance and both states give a tiny difference in the resonance energies but the 2^- state has a width larger than the 0^- state has. All of the potentials give less than 1 MeV as the resonance energies of both states. As for the width, the FU gives the largest width, $\Gamma_R = 6.6$ MeV for the 0^- state and 8.2 MeV for the 2^- state, and the CL the smallest width, $\Gamma_R = 1.1$ MeV for the 0^- state and 2.6 MeV for the 2^- state. The F-wave gives three resonance states of 2^-, 3^-, and 4^-, all of which concentrate within 2 MeV in the resonance energy. With the MN, FU, and MH potentials, resonance energies of the three F-wave states are 11–14 MeV while widths are 17–19 MeV for the 2^- and 3^- states and 10–11 MeV for the 4^- state. The CL potential gives smaller resonance energies (6–8 MeV) and widths (9–16 MeV) in comparison with other three potentials. We would like to remark that, among the resonance parameters given in Tables I–IV, the MN and FU potentials give the lower resonance energy in the 2^- state than that in the 0^- state whereas the 2^- state has the broader width than the 0^- state has, as easily seen in Fig. 2. Moreover, the FU potential gives the negative energy ($E_R = -0.6$ MeV) in the 2^- state while this is the resonance state($\Gamma_R = 8.2$ MeV). We can understand this behavior for these two P-wave resonances if we consider on the complex momentum plane. When we assume the complex momentum as $k = \sqrt{E_R - i\Gamma_R/2}$, the MN gives $k = 1.2 - \imath\ 0.9$ for the 0^- and $k = 1.3 - \imath\ 1.1$ for the 2^-. That is, the 2^- state, which has a weaker P-wave attraction between the two triton than the 0^- state, has the larger Re[k] and Im[k] than the 0^- state has, that is quite normal behavior as the S-matrix pole trajectory on the complex momentum plane. For the FU potential, the 0^- state gives $k = 1.3 - \imath\ 1.3$ and the 2^- gives $k = 1.3 - \imath\ 1.5$ which are as well normal behavior and lie on the fourth quadrant on the complex momentum plane. Therefore, this behavior for the resonance energy E_R for the two P-wave resonance states come simply from the larger imaginary part of the complex momentum than the real part.

Concerning the $T = 1$ isobaric analog states in ^{6}Be and ^{6}Li, we confirmed the results consistent with those of ^{6}He as given in Tables I–IV. In ^{6}Be, it should be noted that the ^{3}He+^{3}He resonance state near the threshold can be expected to play an important role in the ^{3}He(^{3}He,$2p$)^{6}Be astrophysical low-energy reaction which is a dominant reaction of the ^{4}He source in stars and competes the ^{3}He(^{4}He,γ)^{7}He reaction in the $p+p$ chain [37]. A few decades ago, a hypothetical narrow resonance locating close to the two-body threshold, which could give an observable enhancement in ^{3}He(^{3}He,$2p$)^{6}Be reaction rate and some explanation for the missing ^{8}B solar neutrino flux, was suggested [38]. However, theoretical calculations in RGM and GCM [39,40], as well as the experimental search [41], so far did not find any narrow low-energy resonance which could enhance the reaction. Therefore the P-wave resonances obtained in the present study is unlikely to affect the ^{3}He(^{3}He,$2p$)^{6}Be reaction rate since these resonances have very large decay widths ($\Gamma_R = 1.9$–10 MeV).

As it is mentioned in Sec. I, the spin-orbit and tensor terms, which is not included in the preceding theoretical studies [7,10], are taken into account in the our effective nucleon-nucleon interactions. In order to examine the roles of the spin-orbit and tensor terms in the effective nucleon-nucleon interaction for the $T = 1$ odd-wave resonances, we have again calculated the odd-wave phase shifts in ^{6}He but omitting the spin-orbit and/or tensor terms so as to compare these with those in Fig. 2. The calculated phase shifts of the 0^- and 4^- states with the MN potential are shown in Fig. 3, where those which omit the spin-orbit and tensor terms are given by the solid lines, those which omit the tensor term are by the dotted lines, and those with the spin-orbit and tensor terms are by the dashed lines. Results which is consistent with those by the MN potential are obtained by the other three potentials. We can see in the 0^- state, which is the narrowest resonance among the P-wave states, that the tensor term gives an important role to make this resonance narrower while the spin-orbit term gives a less important role. In the 4^- state, which is the narrowest resonance among the F-wave states, the spin-orbit term enhance largely this phase shift while the tensor term enhance a little. In the other P- and F-wave resonances of the 1^-, 2^-, and 3^- states, both terms give smaller contributions or repulsive effects. Therefore, above results show the important role of the tensor term for the 0^- P-wave resonance and of the spin-orbit term for the 4^- F-wave resonance.

For the $T = 0$ states in ^{6}Li, $t+h$ elastic scattering phase shifts in positive parity states are shown in Fig. 4, where four states of $^3S_1$,$^3D_1$,$^3D_2$, and $^3D_3$ are given by the solid, dotted, dashed, and dash-dotted lines, respectively. This figure shows that 1^+ states in the S- and D-waves (solid and dotted lines) do not give any sign of the resonance states. The D-wave phase shifts of 2^+ and 3^+ (dashed and dash-dotted lines) show a

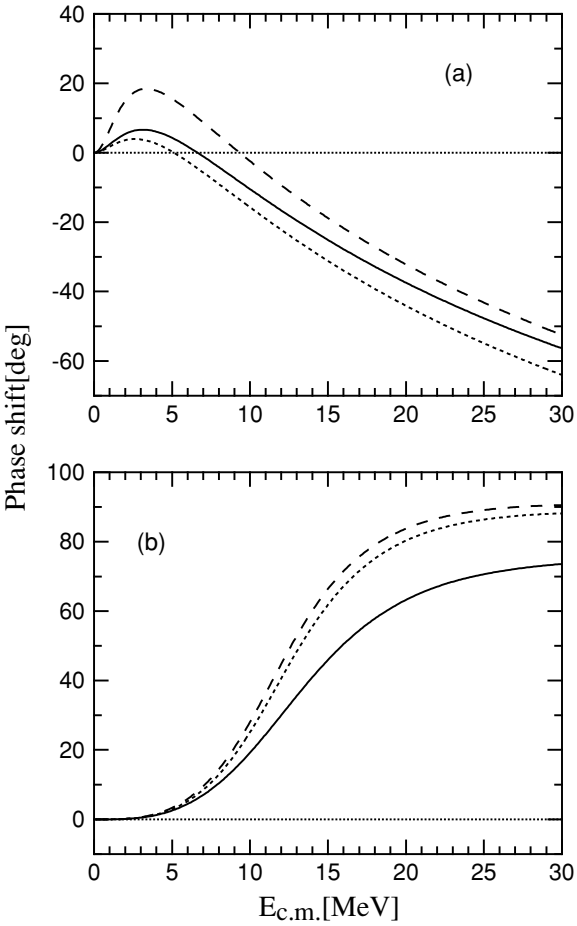

FIG. 3. t+t elastic phase shifts of the (a) 0^- and (b) 4^- states in ^{6}He. The MN potential is used as the effective N-N potential. The solid, dotted, and dashed lines are the results without the spin-orbit and tensor terms, without the tensor term, and with spin-orbit and tensor terms, respectively.

very small peak which implies an existence of the very broad resonance, but they have apparently certain dependence upon the employed interaction. Note that these 2^+ and 3^+ resonance states require excitation more than $2\hbar\omega$ so as to be produced in the shell model since the first states of 2^+ and 3^+ are obtained as deeply bound states as discussed below. Therefore it could have some uncertainty to discuss these D-wave resonances within the present t+t cluster model and further extension of the model space might be desired in order to get more reliable resonance parameters.

Concerning the negative parity states ($T = 0$), t+h phase shifts are shown in Fig. 5, where the P- and F-waves are given by the solid and dotted lines, respectively. A P-wave phase shift (1^-) gives a small peak below 5 MeV except the FU potential. The FU has, in the $T = 0$ state, the weakest attraction for cluster relative motion while the CL has the strongest attraction as is in the $T = 1$ state. An F-wave phase shift (3^-) shows a very broad resonance lying at much higher energies than the P-wave resonance lies.

The resonance parameters for these $T = 0$ states obtained by the ACS are given in a lower part of Tables I–IV. Our model gives, in every interaction, four bound states with the positive parity, two in the 1^+ state and one in each of 2^+ and 3^+ states, but no bound state is found in the negative parity state. ^{6}Li is experimentally known to have the ground state of 1^+ and excited states of $3^+(E_x = 2.2$ MeV), $2^+(E_x = 4.3$ MeV), and $1^+(E_x = 5.7$ MeV), while the t+h threshold lies at $E_x = 15.8$ MeV [2]. And these low-lying states are considered to be dominated by the α+p+n or $\alpha + d$ structure. Note that, in an $\alpha + d$ configuration, the S-wave state gives a spin-parity of 1^+ and the D-wave gives of 1^+, 2^+, and 3^+ and the present calculation, in fact, shows an S-wave dominance for the lowest 1^+ state and a D-wave for others. We have calculated the t+h reduced width amplitudes in these bound states as was done in ^{6}He, and the node and the partial wave of these amplitudes indicate that these states are dominated by the $0\hbar\omega$ excitation in the shell model configuration. According to above facts, it is quite natural to consider these bound states being experimentally known states of 1^+_1, 3^+, 2^+, and 1^+_2 lying below $E_x < 6$ MeV. A certain overlap between the t+h and α+p+n (or $\alpha + d$) configurations makes these four states being the bound states as is found in the $T = 1$ case. Among these states, the second 1^+ state has much higher excitation energy than others whereas an experimental excitation energy of the second 1^+ is 5.7 MeV [2]. One of possible explanations is that the α+p+n ($\alpha + d$) configuration of this second 1^+ state has much less overlap with the t+h configuration than others have, that is, the wave function of this state is much less spatially localized than other three states.

In odd-wave resonance states, the parameters of P- and F-wave resonances in the $T = 0$ state are very close to those in the $T = 1$ state except the FU potential, because the central part of the present interaction except the FU potential hardly changes these odd-wave phase shifts between $T = 0$ and 1. Note that when the y defined in Refs. [7,10] go to 1.0 ($w = m$ and $b = h$), both odd-wave phase shifts agree exactly and the MH potential used here is in this case.

Comparing our resonance parameters of ^{6}Li with other theoretical calculations, our results seem to be consistent with those by Ohkura *et al.* [10] who employed the CSM in the RGM calculation. They gave $E_R = 1.3$ MeV (1.1 MeV) and $\Gamma_R = 4.4$ MeV (5.5 MeV) for the ^1P (^3P) state and $E_R = 10.1$ MeV (10.7 MeV) and $\Gamma_R = 9.6$ MeV (11.2 MeV) for the $^1F(^3F)$ state. On the other hand, our resonance energies in the P-wave states are a few MeV lower than those by Thompson and Tang [7] who used one-level formula for their calculated phase shifts. They gave $E_R = 5.5$ MeV (6.5 MeV) and $\Gamma_R = 6.9$ MeV (9.3 MeV) for the ^1P (^3P) state and $E_R = 13.0$ MeV (14.0 MeV) and $\Gamma_R = 5.9$ MeV (7.5 MeV) for the $^1F(^3F)$ state. Concerning this discrepancy, it must be mentioned that the definition of the resonance parameters in the ACS and the CSM is different from that in the phase shift analysis. Resonance parameters in the ACS and the CSM are determined by the position of the S-matrix pole on the complex energy (momentum) plane whereas the parametrization by the phase shift analysis is based on the real energy axis. When a resonance state has a small width, that is, the S-matrix pole lies near the real energy axis, both methods can give quite similar results, however, once the S-matrix pole moves far from the real energy axis, we can find some discrepancies in

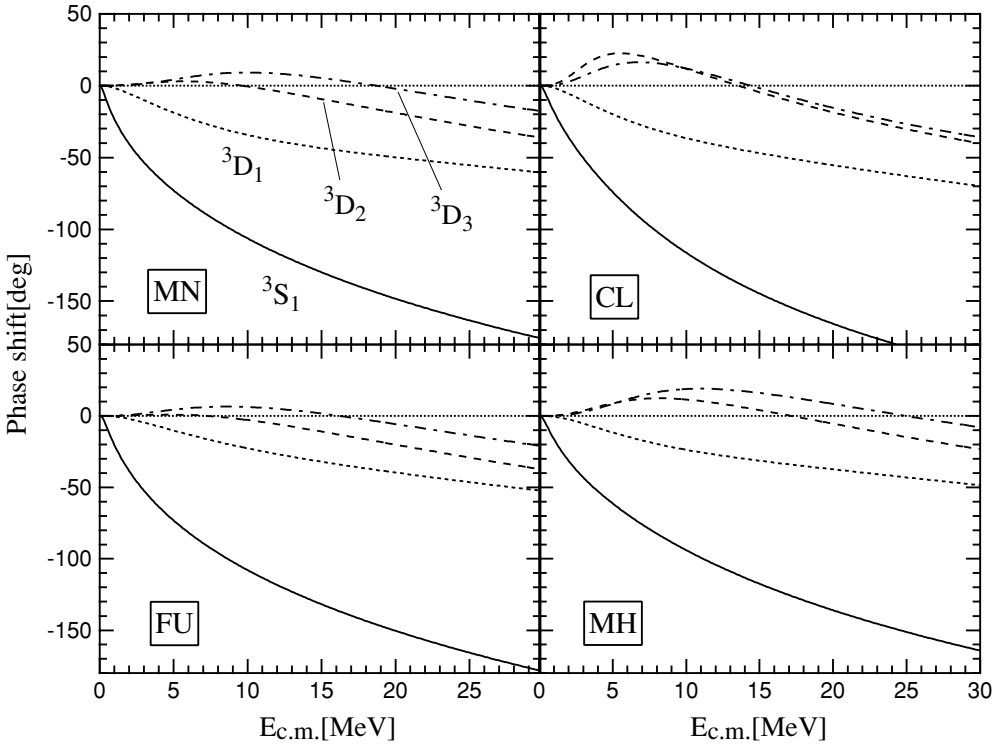

FIG. 4. $t+h$ elastic phase shifts for the positive parity states in ^{6}Li. This is given as a function of the c.m. energy with respect to the $t+h$ threshold. The phase shifts of $^3S_1, ^3D_1, ^3D_2$, and $^3D_3$ are given by the solid, dotted, dashed, and dash-dotted lines, respectively.

their parameters due to the different definition of the resonance parameters, as is seen in Table I of Ref. [35]. This can be applied when our results is compared with the experimental data, especially for broad resonances.

Secondly comparing with the experimental data, the recent experiments in Ref. [3] gave P-wave resonances without spin assignment in the $A = 6$ systems as $E_R = 5.7\pm1.0$ MeV and $\Gamma_R = 9.5\pm1.0$ MeV for ^{6}He, $E_R = 6.2\pm1.0$ MeV and $\Gamma_R = 8\pm1$ MeV for ^{6}Li($T = 1$), $E_R = 2.2\pm0.5$ MeV and $\Gamma_R = 5.0\pm0.5$ MeV for ^{6}Li($T = 0$), and $E_R = 6.5\pm1.2$ MeV and $\Gamma_R = 9.2\pm1.3$ MeV for ^{6}Be. On the whole our results give smaller resonance energies and widths. Most noticeable difference between our results and recent experimental data [3] can be found in an energy difference of the P-wave resonance between the $T = 0$ and 1 states in ^{6}Li. As mentioned above, our results with three potentials other than the FU potential give less than 1 MeV as the energy difference whereas the experimental data give about 4 MeV. And, comparing with other experiments in Refs. [4–6], they gave 2^- or 0^- as spin assignments of the $T = 1P$-wave resonances [5,6] and this is consistent with our results since our present model cannot give clear evidence of the 1^- resonance. In $T = 1F$-wave resonances, Mondragón [6] gave three resonances in ^{6}Li and Vlastou [5] gave as well three in ^{6}Be as gives our calculation, while Ventura [4] gave two (3^- and 4^-) in ^{6}Li and one (3^-) in ^{6}Be and Vlastou [5] gave two (3^- and 4^-) in ^{6}Li. Mondragón [6] gave, in the $T = 1$ states of ^{6}Li, not only resonance energies but also widths, $E_R = 2.190$ MeV and $\Gamma_R = 3.012$ MeV for the 2^-(P-wave), $E_R = 10.795$ MeV and $\Gamma_R = 8.684$ MeV for the 2^-(F-wave), $E_R = 8.984$ MeV and $\Gamma_R = 6.754$ MeV for the 3^-, and $E_R = 9.095$ MeV and $\Gamma_R = 5.316$ MeV for the 4^-. On the whole our results are not far from their resonance energies but the widths are much larger than theirs.

IV. SUMMARY

We have explored theoretically the highly excited states of ^{6}He, which have possibly di-triton clustering, by means of the $t+t$ microscopic cluster model. We tried four different effective nucleon-nucleon interactions in order to check the sensitivity to our results and we obtained fairly consistent results in most resonance states. Other members of the $T = 1$ isobaric analog states in the $A = 6$ systems and the $T = 0$ states in ^{6}Li have been as well calculated in consistent ways.

In $T = 1$ P-waves, we have obtained rather broad resonances just above the two-body threshold wherein the 0^- resonance is most noticeable and the 2^- resonance lies quite close to the 0^- state but with a broader width. Our model implies that the 1^- state is unlikely to be observed experimentally as a P-wave resonance. In $T = 1F$-waves, three overlapping resonances of 4^-, 3^-, and 2^- have been obtained with much higher energies and broader widths than those of the P-wave resonances. Among these resonances, the tensor term in the effective nucleon-nucleon interaction plays an important role for the narrowest P-wave resonance of the 0^- state and for the narrowest F-wave resonance of the 4^- state it is the spin-orbit term. In $T = 0$ states in ^{6}Li, resonance energies of single P- and F-wave resonances are very close to those in $T = 1$ states.

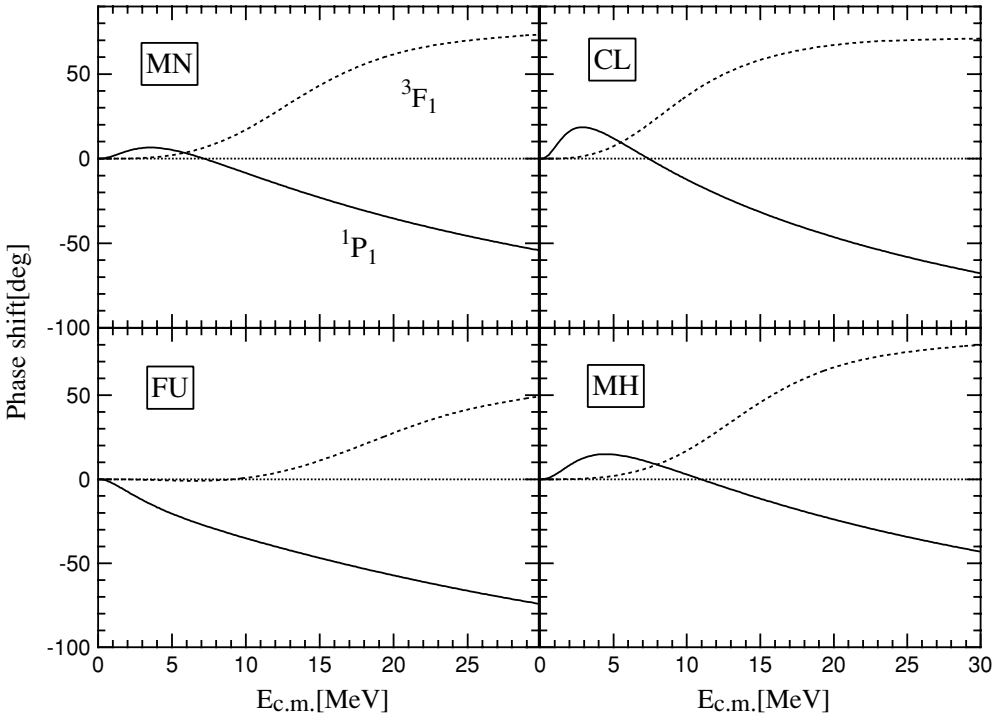

FIG. 5. $t+h$ elastic phase shifts for the negative parity states in ^{6}Li. The phase shifts of $^1P_1$ and $^1F_3$ are given by the solid and dotted lines, respectively.

In comparison with other theoretical studies, our results are close to those by Ohkura *et al*. [10] but some disagreements are found with those by Thompson and Tang [7], in which they neglected the spin-orbit and tensor terms, naturally due to the different definition of the resonance parameters. With experimental data, our results in P-wave resonances have given lower resonance positions on the whole and a smaller isospin splitting in ^{6}Li than those obtained in recent experiment by Akimune *et al*. [3]. In $T = 1$ F-wave resonances of ^{6}Li, our resonance widths are on the whole much broader than those by Mondragón [6].

Finally, we would like to mention that the present model employs the simple $(0s)^3$ function as the triton or ^{3}He cluster internal function whereas, in reality, the triton wave function has a D-wave mixture about 9% [42]. Accordingly, in the effective $N+N$ interaction employed here, the contribution of the tensor term is partly included into the central term. Therefore, more realistic cluster internal function with the more realistic $N+N$ interaction is desired for full understanding the the contribution of the non-central potential for the $t+t$ resonance. Although such an extend calculation in the microscopic cluster model is intriguing and challenging, this is beyond the scope of the present paper.

ACKNOWLEDGMENTS

K.A. acknowledges Dr. A. Csótó for helpful discussions about the Minnesota potential. This work was supported in part by Grant-in-Aid for Scientific Research (Grant No. 17740137) from the Ministry of Education, Science and Culture.

[1] I. Tanihata, J. Phys. G **22**, 157 (1996).
[2] D. R. Tilley *et al*., Nucl. Phys. **A708**, 3 (2002).
[3] H. Akimune *et al*., Phys. Rev. C **67**, 051302(R) (2003); S. Nakayama *et al*., *ibid*. **69**, 041304(R) (2004); T. Yamagata *et al*., *ibid*. **71**, 064316 (2005).
[4] E. Ventura, J. R. Calarco, W. E. Meyerhof, and A. M. Young, Phys. Lett. **B46**, 364 (1973); E. Ventura, C. C. Chang, and W. E. Meyerhof, Nucl. Phys. **A173**, 1 (1971); E. Ventura, J. Calarco, C. C. Chang, E. M. Diener, E. Kuhlmann, and W. E. Meyerhof, *ibid*. **A219**, 157 (1974).
[5] R. Vlastou, J. B. A. England, O. Karban, and S. Baird, Nucl. Phys. **A292**, 29 (1977); R. Vlastou, J. B. A. England, O. Karban, S. Baird, and Y.-W. Lui, *ibid*. **A303**, 368 (1978).
[6] A. Mondragón and E. Hernábez, Phys. Rev. C **41**, 1975 (1990).
[7] D. R. Thompson and Y. C. Tang, Nucl. Phys. **A106**, 591 (1968); Phys. Rev. **159**, 806 (1967).
[8] K. Langanke, in *Advances in Nuclear Physics*, Vol. 21, edited by J. W. Negele and E. Vogt (Plenum, New York, 1994), p. 85.
[9] K. Wildermuth and Y. C. Tang, *A Unified Theory of the Nucleus* (Vieweg, Braunschweig, 1977).
[10] H. Ohkura, T. Yamada, and K. Ikeda, Prog. Theor. Phys. **94**, 47 (1995).
[11] Y. K. Ho, Phys. Rep. **99**, 1 (1983).
[12] N. Moiseyev, Phys. Rep. **302**, 212 (1998).
[13] P. G. Hansen and B. Jonson, Europhys. Lett. **4**, 409 (1987).
[14] K. Ikeda, INS Report JHP-7, 1988;Nucl. Phys. **A538**, 355c (1992).
[15] S. Nakayama *et al*., Phys. Rev. Lett. **85**, 262 (2000).

[16] Y. Suzuki, Nucl. Phys. **A528**, 395 (1991).
[17] A. Csótó, Phys. Rev. C **49**, 3035 (1994).
[18] S. Aoyama, S. Mukai, K. Katō, and K. Ikeda, Prog. Theor. Phys. **93**, 99 (1995).
[19] S. Aoyama, Phys. Rev. C **68**, 034313 (2003).
[20] A. Csótó, Phys. Rev. C **48**, 165 (1993).
[21] K. Arai, Y. Suzuki, and R. G. Lovas, Phys. Rev. C **59**, 1432 (1999).
[22] D. Baye, P.-H. Heenen, and M. Libert-Heinemann, Nucl. Phys. **A291**, 230 (1977).
[23] H. Kanada, T. Kaneko, S. Saito, and Y. C. Tang, Nucl. Phys. **A444**, 209 (1985).
[24] D. R. Thompson, M. LeMere, and Y. C. Tang, Nucl. Phys. **A286**, 53 (1977).
[25] I. Reichstein and Y. C. Tang, Nucl. Phys. **A158**, 529 (1970).
[26] P. Heiss and H. H. Hackenbroich, Phys. Lett. **B30**, 373 (1969).
[27] A. Csótó, R. G. Lovas, and A. T. Kruppa, Phys. Rev. Lett. **70**, 1389 (1993); A. Csótó, H. Oberhummer, and R. Pichler, Phys. Rev. C **53**, 1589 (1996); A. Csótó and G. M. Hale, *ibid.* **55**, 2366 (1997).
[28] A. Csótó and R. G. Lovas, Phys. Rev. C **46**, 576 (1992).
[29] H. Furutani, H. Horiuchi, and R. Tamagaki, Prog. Theor. Phys. **62**, 981 (1979).
[30] T. Mertelmeier and H. M. Hofmann, Nucl. Phys. **A459**, 387 (1986).
[31] D. R. Tilley, H. R. Weller, and G. M. Hale, Nucl. Phys. **A541**, 1 (1992).
[32] K. Arai, P. Descouvemont, and D. Baye, Phys. Rev. C **63**, 044611 (2001).
[33] I. J. Thompson and A. R. Barnett, Comput. Phys. Commun. **36**, 363 (1985); J. Comput. Phys. **64**, 490 (1986).
[34] A. G. M. van Hees and P. W. M. Glaudemans, Z. Phys. A **315**, 223 (1984).
[35] A. Csótó and G. M. Hale, Phys. Rev. C **55**, 536 (1997).
[36] Y. Suzuki, K. Arai, Y. Ogawa, and K. Varga, Phys. Rev. C **54**, 2073 (1996).
[37] C. E. Rolfs and W. S. Rodney, *Cauldrons in the Cosmos* (University of Chicago Press, Chicago, 1988).
[38] V. N. Fetisov and Y. S. Kopysov, Phys. Lett. **B40**, 602 (1972); Nucl. Phys. **A239**, 511 (1975).
[39] P. Descouvemont, Phys. Rev. C **50**, 2635 (1994).
[40] A. Csótó and K. Langanke, Nucl. Phys. **A646**, 387 (1999).
[41] C. Arpesella *et al.*, Phys. Lett. **B389**, 452 (1996); M. Junker *et al.*, Phys. Rev. C **57**, 2700 (1998).
[42] R. Tilley, H. R. Weller, and H. H. Hasan, Nucl. Phys. **A474**, 1 (1987).